Bubble Generation by Micro-Orifices with Application on Activated Sludge Wastewater Treatment

Mohseni, E.; Herrmann-Heber, R.; Reinecke, S. F.; Hampel, U.;

Originally published:

April 2019

Chemical Engineering and Processing: Process Intensification 143(2019), 107511

DOI: https://doi.org/10.1016/j.cep.2019.04.011

Perma-Link to Publication Repository of HZDR:

https://www.hzdr.de/publications/Publ-28585

Bubble Generation by Micro-Orifices with Application on Activated Sludge Wastewater Treatment

E. Mohseni[1], R. Herrmann-Heber[2], S.F. Reinecke[2], and U. Hampel[1,2]

[1] AREVA Endowed Chair of Imaging Techniques in Energy and Process Engineering,

Technische Universität Dresden, Dresden, 01062, Germany (e-mail: *ehsan.mohseni@tu-dresden.de; uwe.hampel@tu-dresden.de*)

[2] Helmholtz-Zentrum Dresden-Rossendorf, Institute of Fluid Dynamics, Bautzner Landstraße 400,

01328 Dresden, Germany (e-mail: *s.reinecke@hzdr.de; r.herrmann-heber@hzdr.de*)

Abstract

We studied the initial gas dispersion performance of diffuser concepts based on micro-orifices and needles with very fine orifice diameters in the range from 30 µm to 200 µm, as such diffusers are currently in discussion for energy-efficient wastewater treatment plants. To evaluate the performance of these micro-orifices, we compared them with industrial rubber membrane diffusers with respect to Sauter mean bubble diameter, pressure drop, frequency of bubble formation, oxygen transfer rate, and power demand for air compression. Our study revealed that, in comparison with rubber membrane diffusers, bubbles generated from the micro-orifices transfer up to 82% more oxygen content into the continuous phase at up to 75% less power demand. Moreover, these micro-orifices are able to produce bubble sizes in the same range as the needle diffusers at 60% less pressure drop and 60% higher bubble generation frequency. Therefore, we also expect an improvement in the oxygen transfer coefficient $K_L a$ and standard oxygen transfer efficiency *SOTE* compared to commercial rubber membrane diffusers.

Graphical Abstract

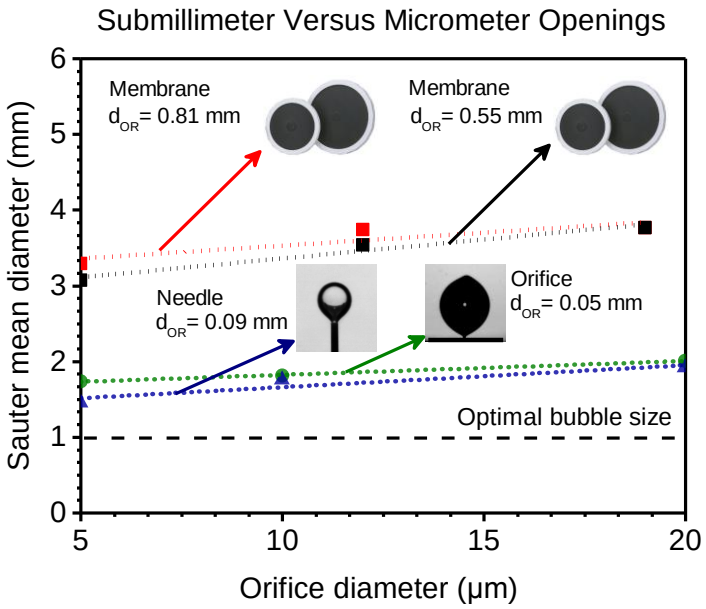

Highlights

- Micro-orifices have a good potential to improve the performance of an aeration process
- Air compression power demand reduces up to 75% using micro-orifices
- Oxygen transfer rate is 22% higher for micro-orifices than for submillimeter ones
- Small bubbles generated by needle diffusers can be reproduced by micro-orifices
- To produce optimal bubble size, an external bubble detachment mechanism is required

Keywords: Bubble Generation, Micro-orifices, Aeration, Biological Wastewater Treatment, Rubber Membrane Diffusers, Oxygen Transfer

1. INTRODUCTION

Gas bubble dispersion plays a significant role for mass transfer, mixing and product quality in a large number of chemical, biochemical, and other processes [1-4]. Of particular importance is the dispersion of air bubbles, known as aeration process, in the activated sludge basins in biological wastewater treatment plants (WWTP) [5]. The aeration process provides an aerobic environment for microbial degradation of organic matters. Moreover, it enhances the homogeneity in the basin, which improves contacting of microorganisms with dissolved and suspended organic matter. To maintain aerobic conditions and the suspension of activated sludge, oxygen in a form of air bubbles is continuously supplied to the aeration basin. This takes the largest share of energy bill in the whole WWTP in the range of 45% to 75% [6].

State of the art of aerators are rubber membrane diffusers, which offer relatively low standard oxygen transfer efficiency *SOTE* in the order of 40% to 60% [7]. Various factors, such as the gas holdup, bubble size, bubble residence time, and apparent viscosity, affect the *SOTE* of a system [8-10]. Among these parameters, the bubble size is of great importance, as it directly determines the gas holdup and the bubble residence time. Moreover, the bubble size defines the surface area to volume ratio, which affects the oxygen transfer rate *OTR* and the oxygen absorption. As pointed out by Motarjemi and Jameson [10], it is e.g. required to produce air bubbles in the range of 0.7 mm to 1.0 mm to achieve 95% oxygen absorption for a typical submergence of 3 m to 6 m in the basin. However, rubber membranes diffusers typically produce bubbles in the order of 3 mm to 5 mm, which results in a limitation of the oxygen absorption from the injected air bubbles below 50% [11, 12]. Moreover, due to their geometry they produce larger bubbles at the centre of the diffuser and hence promote a non-uniform radial bubble distribution. This maldistribution leads to development of two regions of low and high mixture density above the middle and the circumference of the diffuser respectively. Eventually, this results in radial movement of both the continuous and dispersed phases toward the centre and enhances the coalescence rate. Therefore, it is valuable to reduce the bubble size and make the radial gas holdup profile uniform to limit the bubble interaction and thus enhance the diffuser performance.

Various parameters are involved in the process of bubble formation. The effect of these parameters has been discussed by different authors in detail [13, 14]. Generally, one can group up these parameters into three categories: equipment variables, system variables, and operation variables. Equipment variables include parameters such as the diameter,

geometry, arrangement and orientation of the orifice as well as the gas reservoir underneath of the orifice. Factors associated with continuous and dispersed phases, namely surface tension, density of liquid and gas phase, three-phase contact angle, and velocity of sound in the gas, are assigned under the category of system variables. Finally, the operation variables are those, which are defined by the operator, such as the volumetric gas flow rate, velocity of continuous phase, submergence, pressure drop and temperature.

By changing these parameters, formation of bubbles from a single submerged orifice can occur in different regimes. According to McCann and Prince, there are three accepted regimes of bubbling, namely quasi-static, dynamic and jetting [15]. They mainly depend on the orifice configuration, gas velocity, submergence, gas-liquid system properties, and the magnitude of gravitational force acting on the system. Bubbles generated at an orifice under quasi-static conditions have almost the same size, which is determined by the dominant forces in this regime, i.e. surface tension and buoyancy. Balancing these forces leads to the so-called Fritz volume V_F, where $V_F = \pi\sigma_L d_{OR}/\rho_L g$ [16]. To operate in the quasi-static regime, the gas flow rate should be kept below the critical value of $Q_c \cong \pi(16/3g^2)^{1/6}\ (\sigma_L d_{OR}/2\rho_L)^{5/6}$ or below the critical dimensionless Weber number $We_Q^c = (16/3)^{1/3} Bo^{-2/3}$, as suggested by Oguz and Prosperetti and Bolaños-Jiménez et al. [17, 18], respectively. Here σ_L is the liquid surface tension, d_{OR} is the orifice diameter, ρ_L the liquid density, g the acceleration of gravity, and *Bo* is the dimensionless Bond number, $Bo = \rho_L d_{OR}^2 g/\sigma_L$. These values are corresponding to the transition from the quasi-static regime to the dynamic bubbling regime. Further increase in the gas flow rate results in bubbling in the dynamic regime, where bigger bubbles with a highly dynamic surface are formed. In the dynamic regime, both bubble volume and frequency will change with the gas flow rate. Further increase in the gas flow rate will result in transition to the jetting regime. The latter occurs when two or more bubbles coalesce close to the orifice, rise only a short distance and eventually shatter into undefined number of bubbles of different sizes.

Previous experimental and theoretical investigations are mainly categorized according to three different gas injection conditions, namely, constant flow, constant pressure, and intermediate conditions [19]. This classification highly depends on the volume of the gas reservoir, also known as the chamber volume V_C under the orifice [20-23]. If the volume of the gas reservoir upstream of the orifice is rather large in comparison to the volume of the generated bubble, the varying gas efflux due to formation of a bubble will not significantly change the pressure in the chamber. This corresponds to the situation in which bubbles are

generated under constant pressure conditions. In contrast, if there is a high pressure drop restriction, such as a long capillary between the gas reservoir and the orifice, the bubble formation causes pressure fluctuations but the rate of gas flow through the orifice can be taken as a constant value. However, the pressure fluctuations are much smaller than the pressure drop between the gas reservoir and the orifice. This is called bubble formation under constant flow condition. Intermediate conditions are given when neither the gas flow rate nor the pressure of the chamber remain constant during the bubble formation. Industrial diffusers mainly operate under constant pressure conditions, since it is intended to keep the system pressure as low as possible in conventional aeration systems of WWTP [24]. In the aeration pools, diffusers are directly mounted on a main gas feed line, which makes the chamber volume large enough to satisfy the constant pressure condition. In order to distinguish between these gas injection conditions, Tadaki and Maeda proposed a dimensionless capacitance number N_c, which is the relative importance of the liquid pressure force at the orifice to the reservoir weight, if it would contain liquid [25]. They suggested specific ranges of the capacitance number according to the three gas injection conditions for perforated plates [26]:

$N_C < 1$	for the constant flow condition
$1 < N_C < 9$	for the intermediate condition and
$N_C > 9$	for the constant pressure condition.

In case of capillary pipes, which applies for needle diffusers, the condition of $\frac{L}{d_{OR}^4} > 10^{12}\ m^{-3}$ satisfies the constant flow condition, where L is the length and d_{OR} is the inner diameter of the pipe or needle [27].

Investigation on submillimeter orifices started from early 90's. Teresaka and Tsuge [28] proposed a new criterion for describing the mechanism of bubble formation at orifices with diameters in the range from 0.3 to 3.01 mm. Vafaei et al. [29, 30] and Vafaei and Wen [31] experimentally investigated the bubble growth at stainless steel needles with inner diameters of 0.11, 0.51 and 0.84 mm under low volumetric gas flow rates in the range from 0.015 to 0.83 ml/min. Bubble shape was predicted by solving the Young-Laplace equation and the results were validated experimentally. A multistage bubble growth was recognized, which was forced by the motion of the bubble's contact line to the orifice as well as interacting forces. The relations of bubble detachment volume, detachment time, and waiting time with

orifice diameter of 0.052, 0.12, and 0.5 mm were investigated by Xie et al. 2012 [32]. The inrush of multiple subsequent bubbles into the preceding one was observed for the orifices with 0.12 and 0.054 mm. In a similar attempt, Zhu et al. [33] found a critical gas flow rate of 54 ml/min at which the regime of bubbling switched from single bubbling to non-interval bubbling for 0.054 mm orifice diameter. Simmons et al. [34] simulated the bubble formation using the finite element method and described the global characteristics of the process for a wide range of Ohnesorge numbers, orifice radii and volumetric gas flow rates. The simulation results were observed to agree well with experiments. Zhang et al. 2017 [35] investigated the dynamic behavior of emerging bubbles under low gas flow rates from micro-orifices by means of visualization experiments and numerical simulation. Different nozzles with inner diameter of 0.136, 0.180, and 0.204 mm made of stainless steel were investigated, where gas flow was supplied via a syringe pump. It is reported that the bubble shape was only depended on instantaneous bubble volume and it was independent of gas flow rate.

Rubber membrane diffusers are currently in discussion, as it is necessary to improve their performance in the aeration basins. In recent products, it is tried to achieve smaller bubbles by perforating fine pores with diameters smaller than a millimeter, known as submillimeter range. Only few products are available with micrometer scale perforations and a better performance was achieved in this range [11, 36]. We refer to as the micrometer scale when the diameter of the diffuser is smaller than 300 µm. Such a terminology was also followed by Qu et al. [1]. Despite the current state of the knowledge on bubble formation at micro-orifices, the range of the produced bubble size with respect to the gas flow rate is not known. Moreover, these products are available only with diffusers close to 300 µm. With the current state of manufacturing techniques, it is now economically possible to fabricate small orifices in order of tens of micrometer. However, previous works in bubble formation from a submerged orifice are mainly addressing diffusers above the micrometer range [13, 22, 37]. Hence, leverage of the micrometer orifices on bubble formation is still not sufficiently understood. In our current endeavor, we extended the knowledge about the performance of micrometer diffusers. To be able to operate in a defined gas flow regime, we used a solid orifice geometry. Moreover, as it was not possible to measure in an opaque fluid such as activated sludge by means of optical measurement techniques, we used deionized water and air as continuous and dispersed phase, respectively. Consequently, we could also compare our results with similar works from the literature. We studied two types of solid micrometer diffusers, namely orifices and needles, both made of stainless steel. We characterized the

performance of these diffusers at a similar gas flow rate applied in the aeration basins. We reported the initial bubble size distribution, pressure drop and bubble generation frequency at different flow rates for each diffuser. Finally, we compared the results with commercial rubber membrane diffusers.

2. MATERIALS AND METHODS

2.1. Experimental set-up

A vertical acrylic glass column with rectangular cross section of 250×50 mm^2 and a total height of 1000 mm was placed between a high-speed camera and a light source. The chamber volume under the diffusers was 62×10^3 mm^3. A mass flow controller (FMA 2605A, Omega Engineering Inc.) was used to control the air flow rate with a full-scale range of 50 smL/min and an uncertainty of ± 0.3 smL/min of full scale. Four gas flow rates per orifice were applied, i.e. 5, 10, 20, and 50 smL/min. The pressure drop was measured by means of a relative pressure sensor in the gas reservoir under the orifice with a full-scale range of 600 mbar and an uncertainty of ± 3 mbar. All of the experiments were conducted under constant hydrostatic head of 800 mm deionized water with electrical conductivity of 34.1 µS/cm, at room temperature and atmospheric pressure.

We investigated two types of diffusers, i.e. the orifice and needle diffusers provided by Robert Helwig GmbH and IWWT® GmbH respectively. Needles were made of stainless steel and they were provided in 5 mm and 15 mm length with three different tip inclinations, i.e. 30°, 60°, and 90°. Details about the needle configurations are given in Table 1. Moreover, seven orifices with a range of 30 µm to 200 µm in diameter were also included in our study. The roughness of these diffusers was measured by a Mahr Perthometer M1. The arithmetic average R_Z is given in Table 2 along with the plate thickness *T* and the orifice diameter d_{OR}. The orifices were made on electropolished stainless steel plates using laser processing.

Table 1

Specifications of the needle diffusers.

$No.$	$d_{OR\,in}\ [\mu m]$	$d_{OR\,out}\ [\mu m]$	$Tip\ inclination\ [°]$			$L\ [mm]$	$\frac{L}{d_{OR}^4}\ [m^{-3}]$
N1	90	200		90°		5 , 15	7.6 … 22.8 E+14
N2	120	500	30°	60°	90°	5 , 15	2.4 … 7.2 E+13
N3	150	500	30°	60°	90°	5 , 15	9.8 … 29.6 E+12
N4	200	500	30°	60°	90°	5 , 15	3.1 … 9.3 E+12

Table 2

Specifications of the orifices.

$No.$	d_{OR} $[\mu m]$	T $[\mu m]$	R_Z $[\mu m]$
O1	30	300	0.95
O2	50	300	0.96
O3	70	300	0.98
O4	90	300	1.06
O5	120	500	1.01
O6	150	500	1.03
O7	200	500	1.02

Dimensionless numbers were used to characterize the bubble formation from the diffusers. These numbers are given in Table 3. All N_C values were well above 9, which corresponds to the constant-pressure condition. The constant pressure condition was intentionally maintained in our experimental set-up to mimic the situation in which the rubber membrane diffusers operate in the aeration basins. These commercial aerators are assembled on a large gas reservoir in a form of a pipeline, which results in bubble formation under constant pressure condition. In order to define the bubbling regime for each orifice, the Weber number was calculated, and compared with the critical values suggested by Oguz and Prosperetti [17]. We studied the bubble formation in both the quasi-static regime and the dynamic regime.

Table 3

Dimensionless numbers and critical flow rate for the orifices.

d_{OR} [μm]	N_C	*We*	Q_C [smL/min]	We_Q^c
30	7881.58	2.9E+3 … 2.9E+5	3.9	1.78E+03
50	2837.37	625 … 6.25E+4	6	9.03E+02
70	1447.64	228 … 2.28E+4	7.9	5.76E+02
90	875.73	107 … 1.07E+4	9.8	4.12E+02
120	492.60	45.2 … 4.52E+3	12.5	2.81E+02
150	315.26	23.2 … 2.32E+3	15	2.09E+02
200	177.34	9.77 … 9.77E+2	19.1	1.42E+02

2.2. Image acquisition

The bubble size distribution was measured by means of videometry with the backlight technique. A high-speed camera (MEGA SPEED HHXC X7 PRO) captured images of the bubbles with a frame rate of 500 fps. Backlight was produced by a 200 W LED light source (EVER GmbH). Images represented a 22 mm by 55 mm field-of-view with a resolution of 1920×740 pixels, i.e. a spatial resolution of 29 μm. Exposure time was 500 μs. We measured the initial bubble size distribution 50 mm above the diffuser. The reason was to avoid the error caused by the wobbling of bubble's interface after bubble detachment.

2.3. Image processing

The final bubble volume was measured using an in-house algorithm [38]. In the algorithm, bubble size was determined based on the modified Canny edge detection algorithm [39]. The following processes were carried out: (i) preparation of the original image including correction of the contrast and applying Median and Guassian Filters, (ii) two dimensional derivation, edge thinning and edge selection, (iii) using a hysteresis with two thresholds for the edge selection to obtain weak and strong edges, (iv) closing the edges by simple dilatation and erosion step, (v) identification of inside and outside of the bubble and (vi) finally, filling the structure and calculating the major and minor axis and the area centroid. Main steps of this algorithm are illustrated in Fig.1. The algorithm extracts single bubbles and calculates their equivalent spherical diameter d_E. Finally, each bubble is allocated to a class of a bubble size with 250 μm class width.

Fig. 1. Left to the right: original image; edges detection; filled structures; result with major and minor axis and area centroid.

In each measurement, we processed at least 100 bubbles at low gas flow rates at which bubbles were almost at the same size. At higher flow rates, we observed a bubble size distribution, hence, we measured at least 500 bubbles per measurement. We reported the Sauter mean bubble diameter $d_{32} = \sum_{i=1}^{n} N_i d_E^3 / \sum_{i=1}^{n} N_i d_E^2$ for each diffuser at different gas flow rates. Here d_E is an individual interval of the spherical-equivalent bubble diameter, and

N_i is the number of bubbles within this specific interval [40]. We report the error associated with this sampling to be ±18 μm deviation from the best estimation.

3. RESULTS AND DISCUSSION

3.1. Bubble formation at needle diffusers

3.1.1. *Effect of gas flow rate on bubble size*

Fig. 2 illustrates the performance of the 5 mm long needle diffusers with flat tips (inclination 90°). Smallest bubbles were generated at $Q = 5$ smL/min. In the range $5 < Q \leq 20$ smL/min, d_{32} slightly increased with increasing the diameter. Further increase in the gas flow rate resulted in significant rise in the bubble generation frequency. However, the increase in frequency was less pronounces at bigger needles. We observed the best results at N3, where at much lower pressure drop and higher frequency, bubbles were generated at the same diameter as for the N1. This corroborates the importance of bubble generation frequency in combination with bubble size to provide the effective surface area available for the oxygen mass transfer. Moreover, we acknowledged a notable decrease in the pressure drop, of up to 73% at N3 compared with N1. The same way, the N2 operated at up to 48% lower pressure drop compared with N1. Below 50 smL/min gas flow rate, bubble formation were mainly determined by the bubbling frequency and the pressure drop and not by the initial bubble size. The latter held especially for the needles with inner diameter between 120 µm to 150 µm.

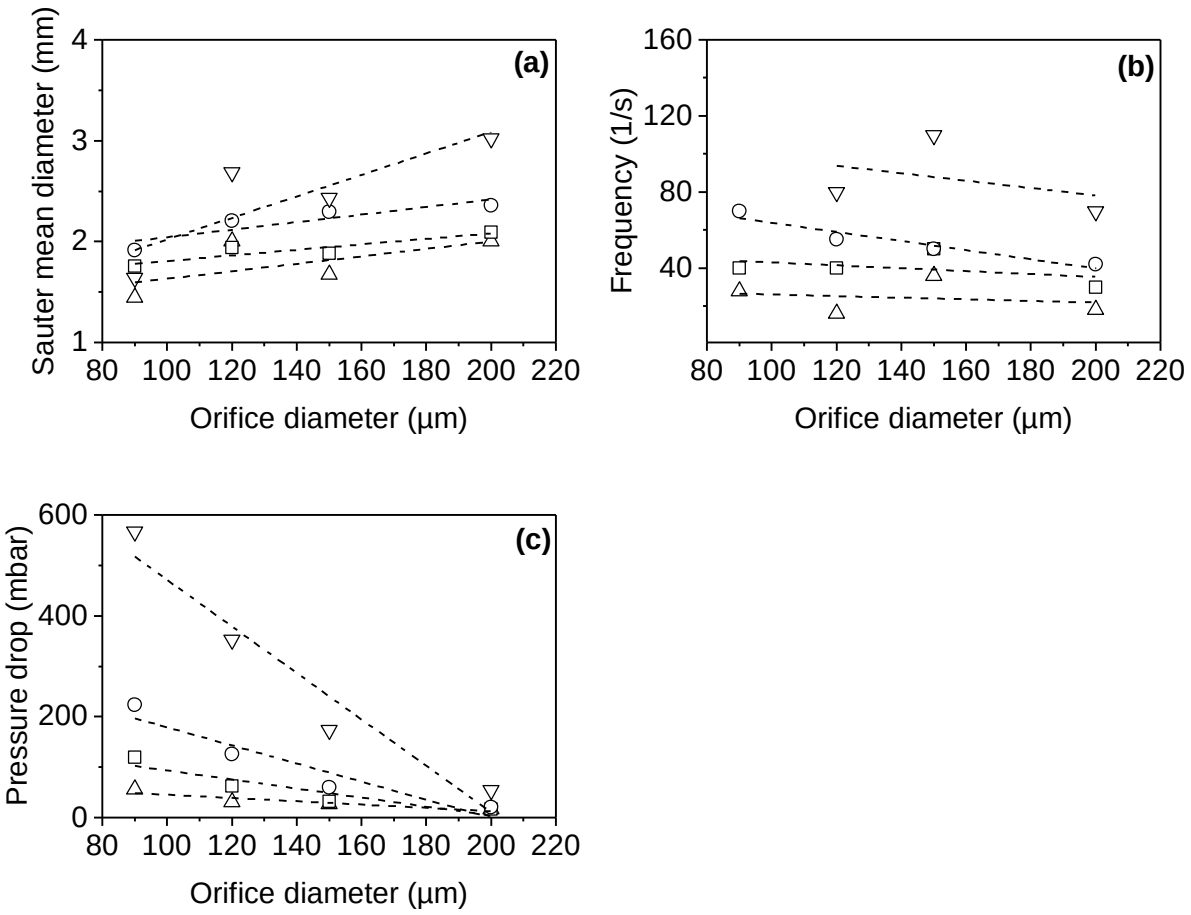

Fig. 2. Graph of (a) the Sauter mean diameter, (b) the bubble generation frequency, and (c) the pressure drop versus the needle's inner diameter for the flat tip needle diffusers with 5 mm length (Legend: △ 5, □ 10, ○ 20, ▽ 50 smL/min).

3.1.2. Effect of the needle tip inclination

As it can be seen in Fig. 3, smaller bubbles were generated from needles with the 30° tip inclination. For the inclined needle tips, the bubble detachment occurred before the expansion of the bubble was completed. This was attributed to the buoyancy-driven sliding movement of the bubble off the orifice's cross section [41]. Compared with the 30° tip inclination, slightly bigger bubbles were generated from the needle with the 60° inclination. The flat tip needles formed the largest bubbles regardless of the gas flow rate. The Sauter mean diameter for needles with tip inclination remained almost constant at gas flow rates below 20 smL/min. However, the frequency increased by a factor of 2.5, when gas flow rate increased from 5 smL/min to 10 smL/min. In this range, the dominant bubbling mechanism was bubbling with single detachment. This situation was favorable to achieve higher surface

area and thus conditions for increased mass transfer. By increasing the gas flow rate, bubbles had less time to slide off from the needle tip. As a result, the preceding bubble was fed by the next one shortly after detachment. Consequently, the detachment was delayed, and the bubble growth was prolonged. The latter was seen at higher gas flow rates (40-50 smL/min) and also observed by Yasuda and Lin [41].

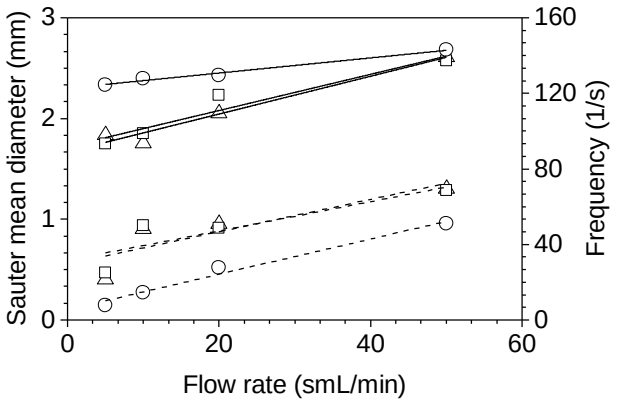

Fig. 3. The Sauter mean diameter and frequency of bubble formation versus gas flow rate for the 15 mm needle with 120 µm inner diameter at different tip inclinations (Legend: △ 30°, □ 60°, ○ 90°, solid lines: Sauter mean diameter, dashed lines: Frequency).

3.1.3. Effect of needle length

We observed a higher-pressure drop when using the 15 mm needles compared with the shorter ones. Pressure drop for 15 mm needles was up to 4.8 times higher than for 5 mm needles. Regarding the bubble size, we noticed that longer needles generate larger bubbles especially at smaller diffusers. Fig. 4 compares the bubble size generated by different needle sizes at 5 and 20 smL/min for both 5 mm and 15 mm needle lengths. We report a similar trend at other gas flow rates. Moreover, Fig. 5 (a) and (b) illustrate the bubble formation from the 5 mm and 15 mm length needles with 120 µm inner diameter. The length scale is comparable, hence, one can observe the bigger bubbles generated from the longer needle compared to the shorter one. This difference is believed to be due to the effect of the capillary length. As described earlier, the correlation proposed by Takahashi was valid in case of 15 mm needles, where due to the relatively high needle length over needle's inner diameter at $d_{OR} < 150$ µm, the gas flow rate through the orifice could be taken as a constant value during bubble formation [27]. In this situation, the effect of the needle length is significant, as

it was also reported by Hayes et al. [42]. Above criterion did not apply at $d_{OR} \geq 150\mu m$. We believe that, the reason of generating smaller bubbles at shorter needles with the same diameter, was attributed to unsteady gas flow feed into the bubble. The latter caused fluctuations on the bubble interface in a form of translating waves toward the bubble apex and back to its base. We did not observe any fluctuation at longer needles, hence, bubbles grew and detached without any external interruption. To have a better comparative perception between needles and orifices, bubble formation from the O5 is also depicted in Fig. 5 (c).

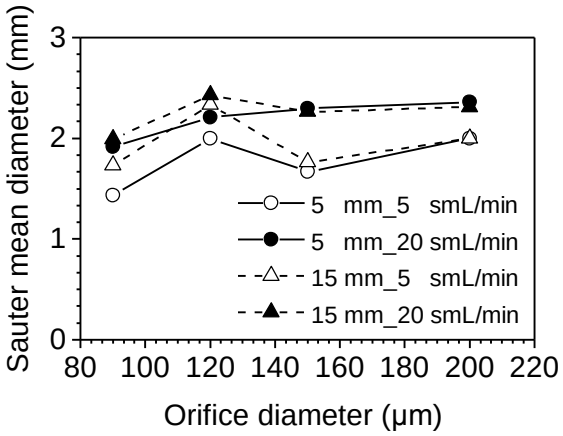

Fig. 4. Comparison of the 5 and 15 mm needle diffusers at 5 and 20 smL/min gas flow rates.

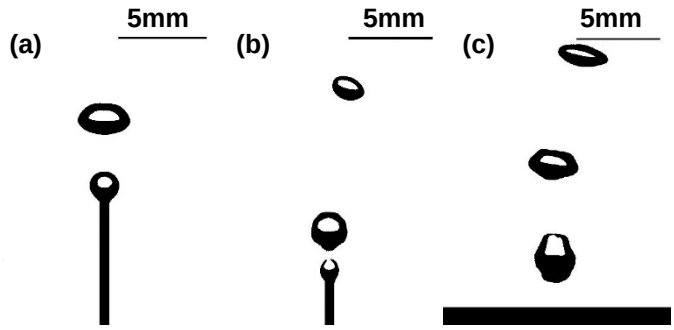

Fig. 5. Bubble formation from the N2 a) 15 mm needle length; b) 5 mm needle length; and c) the O5 all at 10 smL/min gas flow rate.

3.2. Bubble formation at stainless steel orifices

As it can be seen in Fig. 6 (a), at all gas flow rates the Sauter mean diameter increased with increasing the orifice diameter. This trend was descending in case of the bubble generation frequency. The progressive trend of d_{32} by increasing d_{OR} stopped at O4 and O6. At low gas flow rates, bubbles produced at the orifices O2 to O4 were almost the same size. By further increasing the orifice diameter to $d_{OR} = 120$ µm at O5, larger bubbles were generated, which were up to 60% larger than the bubbles generated at the O2 to O4 orifices. Fig. 6 (b) reports the corresponding available surface area, which is calculated from Fig. 6 (a), excluding the influence of coalescence and break-up. It can be seen that the available surface area decreased as the orifice diameter increased at full range of studied gas flow rates. This was due to the significant drop in the frequency of bubble generation.

According to Motarjemi and Jameson, who measured the value of the mass transfer coefficient K_L for oxygen absorption in water, the K_L reaches its maximum when the bubble diameter is about 2 mm [10]. As shown in Fig. 6 (a), the orifices in the range of O2 to O4 generated such a bubble size at 20 smL/min gas flow rate. In addition, to account for the energy consumption for bubble formation from an orifice, one should also consider the variation in the pressure drop as a function of orifice diameter at various gas flow rates. The latter is shown in Fig. 7 that schematically describes the descending trend of the pressure drop by decreasing the gas flow rate and increasing orifice diameter. Combining the data from Figs. 6 and 7, one can comment on the performance of the studied orifices. According to Fig. 6 (b), at O2 to O4, the available surface area decreased at all flow rates. Compared with O2 at 20 smL/min the available surface area decreases in order of 13% and 28%, when using O3 and O4 respectively. The pressure drop at 20 smL/min decreased at O3 and O4 in order of 50% and 63%, when compared with O2, respectively (Fig. 7). On the other hand, pressure drop at 50 smL/min was quite high. Since our focus in the current study is on generating higher available surface area for mass transfer at comparable gas flow rate with rubber membrane diffusers, we nominate O2 and O3 at 20 smL/min gas flow rate as the best candidates among the studied orifices. In the next section, we will compare their performance with the rubber membrane diffusers. It should be mentioned that the smallest bubbles were generated at O1 at $\mathrm{Q} = 5$ smL/min. This value was 1.3 mm at a relatively high pressure drop of 142 mbar.

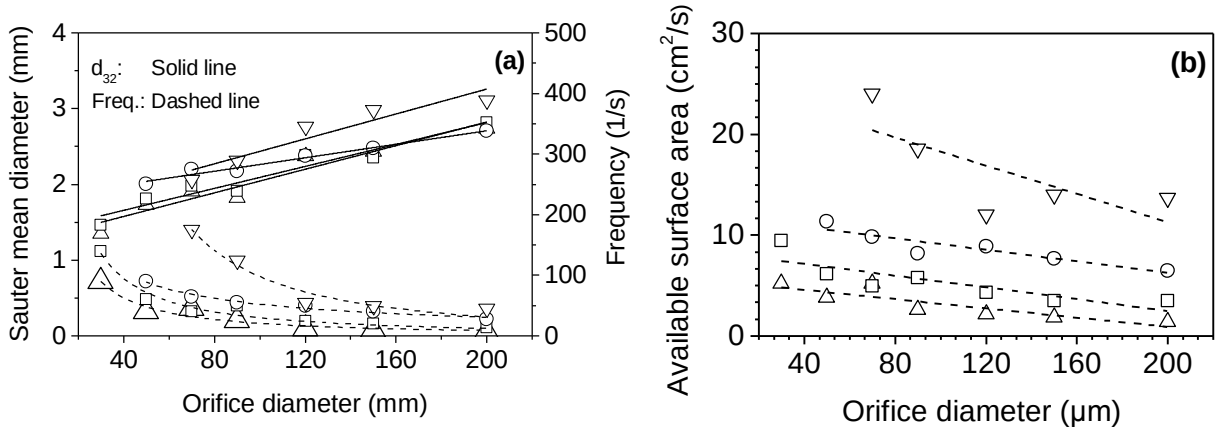

Fig. 6. (a) The Sauter mean diameter and frequency and (b) the available surface area of aeration versus the orifice diameter at different gas flow rates (Legend: △ 5, □ 10, ○ 20, ▽ 50 smL/min).

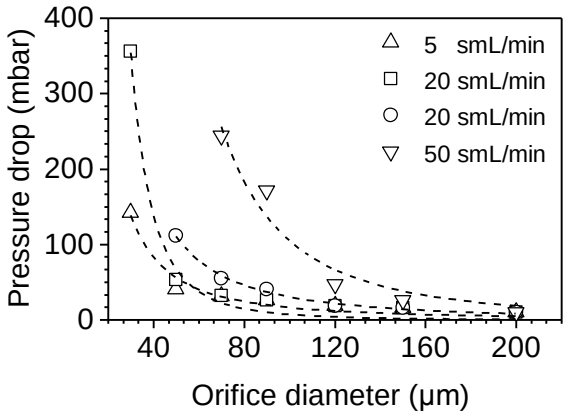

Fig. 7. Pressure drop versus orifice diameter at different gas flow rates.

3.4. Comparison of the diffuser performance

We compared the performance of the investigated diffusers with three industrial rubber membrane diffusers and one flexible orifice. We extracted the information about the rubber diffusers from the available literature [11, 36, 43]. The specification of these rubber membranes is given in Table 4 and the results of this comparison are given in Fig. 8 to Fig. 11. The gas flow rate per orifice was kept consistent at all of the diffusers. To define a comparative range of gas flow rate, we qualitatively tested the bubble formation from the M4. Based on the applied gas flow rate and number of orifices in the M4, we defined the range of 5 – 20 smL/min per orifice. The lowest rate corresponds to the situation, in which, most of the orifices at M4 were engaged with bubble formation. Subsequently, the highest rate represents the bubble formation at all orifices in nearly jetting regime. Deionized water was used as continuous phase; therefore, the change due to the rheological behavior of the liquid phase was negligible. Fig. 8 shows that, the range of bubble sizes generated by the orifices and the needle diffusers were down to 50% smaller than that of the rubber membranes. The orifice M1 generated the same bubbles sizes as the micrometer diffusers. However, this is believed to be due to prevention of normal inflation of this orifice due to blocking of adjacent perforations by a silicone elastomer glue [43]. This is believed to be the reason as the pressure drop of the M1 is also significantly higher compared to the M2 with similar orifice diameter (Fig. 9 (a)). Moreover, Fig. 9 (b) compares the frequency of bubble generation for the same diffusers. As we extracted the data, regarding the rubber membrane diffusers, from literature, we were limited to the available data presented by previous works. Hence, we could only compare the bubble generation frequency of our diffusers with M1. The frequency of bubble generation at M1 was similar to N1 and slightly better than O3. Moreover, O2 has performed significantly better throughout the studied gas flow rates, by generating up to 42% more bubbles at down to 75% lower pressure drop.

Table 4: Specification of the selected rubber membrane diffusers.

No.	Reference	Diffuser Type	d_{OR} [µm]
M1	[43]	Not commercial flexible orifice	600
M2	[11]	ABS Nopon Oy Ltd.	550
M3	[11]	ABS Nopon Oy Ltd.	810
M4	[36]	Sanitaire® Membrane Type SSII	294

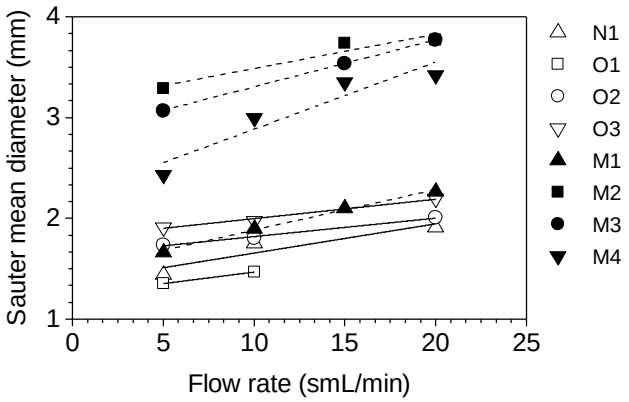

Fig. 8. Comparison of the Sauter mean diameter for the rubber membrane diffusers with selected micrometer diffusers from this study.

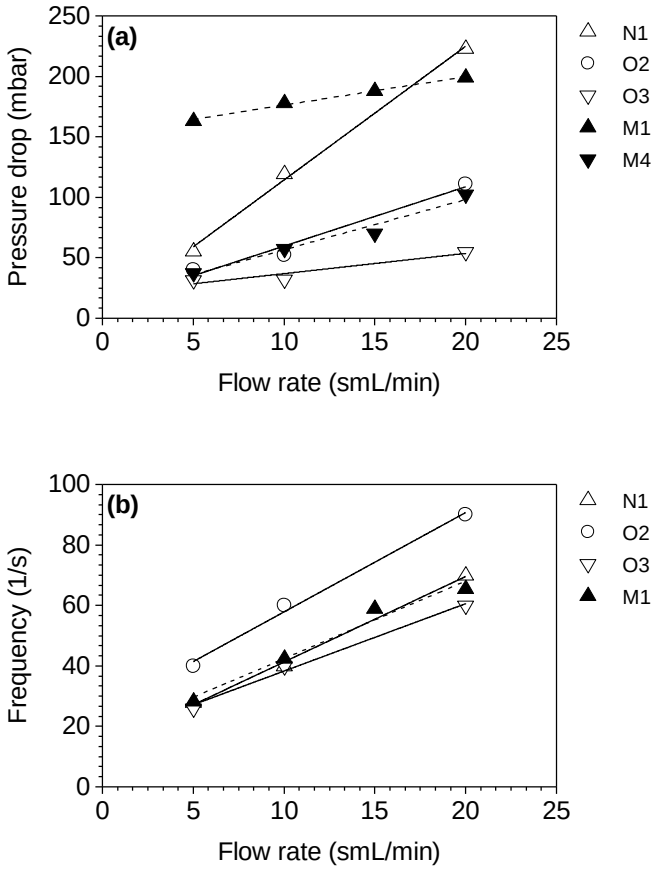

Fig. 9. Comparison of (a) the pressure drop and (b) the bubble generation frequency for the rubber membrane diffusers with a selection of studied solid diffusers.

To estimate the power demand of a blower suitable for such small orifices, here we estimated the equivalent power, which would be needed for the air compression at specific flow rates. We used the empirical equation proposed by Pöpel and Wagner [44]. The latter was derived

from manufacture's data on correlation of equivalent power P in W, as a function of pressure drop, $P = Q_s \cdot E_0 \cdot (h_D + \frac{\Delta p}{98{,}07})^{\Upsilon}$. Here Q_s is the standard gas flow rate in m^3/h, Δp pressure drop in mbar, h_D hydrostatic height in m, E_0 specific energy in Wh/m^4 and Υ empirical exponent. In case of a positive displacement blower, the values of E_0 and Υ are 4.3 and 1, respectively [44]. Fig. 10 compares the power demand per orifice between the investigated diffusers and the flexible ones for a typical hydrostatic height h_D= 0.8 m. At all diffusers, the power demand increased by increasing the rate of gas flow. The M1 demanded the highest rate of power at 5 smL/min, mainly due to its relatively high pressure drop. Although the power demand by N1 was initially lower than M1, at 20 smL/min, N1 claimed almost three times higher power than M1. The demand by O2 and M4 were levelled throughout the studied range of gas flow rates. In comparison with M1 at 5 smL/min, both O2 and M4 required 75% less power demand. The latter was 44% at 20 smL/min. The lowest rate of power demand was measured at O3. Comparing the O3 with commercial rubber membrane diffuser M4, the demand was 15% lower at 5smL/min. However, this value was 51% and 46% less power at 10 and 20 smL/min, respectively. Comparing O3 and flexible orifice M1 at 20 smL/min, the demand of power by O3 was 72% less than M1.

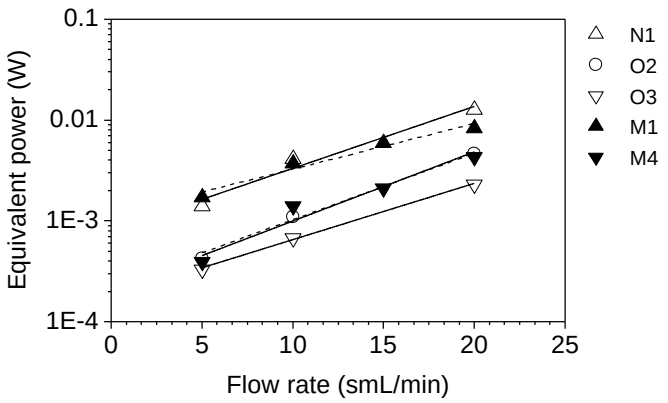

Fig. 10. Comparison of the equivalent power demand to compress the air per orifice.

Motarjemi and Jameson [10] calculated the mass transfer coefficient of wide range of air bubble sizes rising at their terminal velocities in water. They used the measured coefficients to calculate the proportion of oxygen transferred from a defined bubble size, which was released at a given depth in water. The latter was measured for the bubble sizes ranging from 0.3- 5 mm. By extracting this data and using data interpolation at a fixed depth of bubble release, we calculated the amount of oxygen lost from the bubble sizes in our study. Fig.11 (a) and (b), illustrate the proportion of oxygen transfer from air bubbles with defined

diameter as a function of depth at 5 and 20 smL/min gas flow rate, respectively. In both flow rates, by increasing the depth, rate of oxygen transfer has also increased. Bubbles generated at N1 had the highest rate of oxygen transfer compared with other diffusers at all depths. Almost all the oxygen content from these bubbles were transferred, when they were released from 10 m depth. Here, we assume 5 m as the typical depth for aeration basins and we compare the performance at this depth. At 5 smL/min gas flow rate, the least power demanding diffuser, O3, transferred 74% of the oxygen content of generated bubble. The latter was 12% higher than the commercial rubber membrane diffuser M4. Moreover, the transfer rate was levelled for O2 and M1 with the value only 5% higher than O3 in 5 m depth. M2 and M3 had the lowest transfer rate by transferring down to 30 and 28% less oxygen comparing with O3. At 20 smL/min gas flow rate, the overall value of transfer rate was lower than the one at 5 smL/min, as the bubbles were slightly bigger. The rate at N1 was still the highest, although it was 9% lower than transfer rate at 5 smL/min. The difference between O3 and M4, at 20 smL/min, was up to 25% in favor of O3. M2 and M4 had again the lowest rate by only losing 36% of the oxygen content of a bubble released at 5 m depth. As a conclusion, the commercial rubber membrane diffusers with submillimeter openings could not transfer more than 60% of the oxygen content inside the air bubble. This value was up to 82% in case of studied diffusers with micro-meter openings.

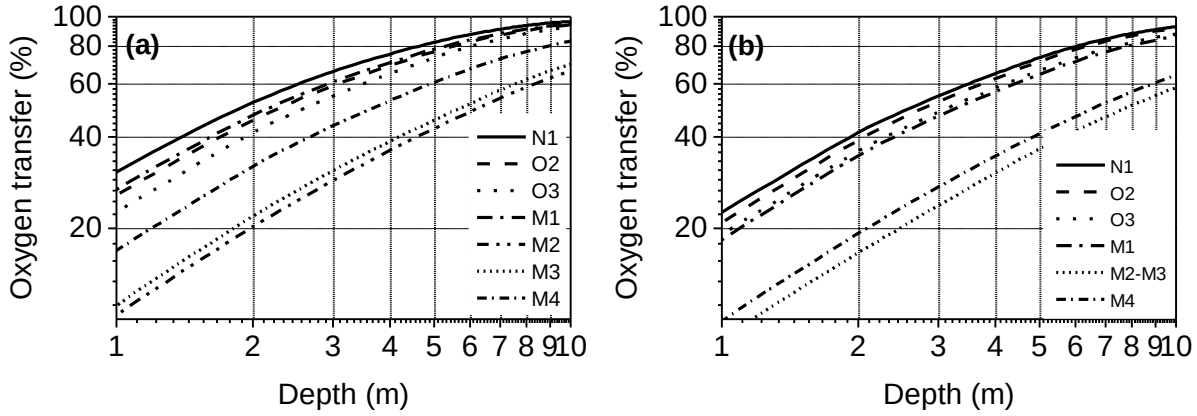

Fig. 11 Ratio of oxygen transferred from air bubbles generated by various diffusers released at different depths at (a) 5 smL/min and (b) 20 smL/min.

4. CONCLUSIONS

Performance of rubber membrane diffusers used in the biological wastewater treatment plants is currently under discussion. Most of the recent products are offered with orifices in the range of submillimeter and only few with micrometer (orifice diameter smaller than 300 µm). However, the performance of these diffusers regarding the generated available interfacial area for mass transfer is still not clear. Available literature mostly addressed the bubble formation from millimeter-orifices and scarce data is available at the smaller range. From the few works available regarding micro-orifices, it is known that, the mechanism of bubble formation from this range is different compared with millimeter orifices. In case of micro-orifices, the final bubble is a product of multiple coalescence of small bubbles in the vicinity above the orifice, which is not the case at millimeter orifices except at sufficiently high gas flow rates. This observation, at micro-orifices, is even valid at very low gas flow rates corresponding to the quasi-static bubbling regime, where a single detachment determines the final bubble volume in case of bigger orifices. To enhance the performance of rubber membrane diffusers, a promising approach would be to use micro-orifices. However, one should characterize the bubble formation from such orifices at comparative gas flow rates applied in the aeration basins. In the current endeavor, we quantitatively analyzed the available interfacial area generated by two types of solid diffusers, i.e. orifice and needle diffusers with micrometer orifice diameters ranging from 30 µm up to 200 µm. Investigated parameters were the Sauter mean diameter, pressure drop, frequency of bubble formation, available surface area, power demand for air compression, and rate of oxygen transfer. To have a comprehensive evaluation, these data were compared with available data from industrial rubber membrane diffusers at the same flow rates.

Orifices in the range of tens of micrometer showed a good potential for improving the aeration performance. Comparing with flexible orifices, bubbles generated from the micro-orifices transferred up to 82% more oxygen content into the continuous phase at up to 75% less power demand. The main advantage of the micro-orifices was generating smaller bubbles at higher frequency of bubble formation. To emphasize the influence of the orifice size we also included needle diffusers into our investigations. However, compared with the best needle performance, O2 generated up to 25% more effective surface area and operated at 50% less pressure drop. Assuming a typical depth of 5 m at aeration basins, it is required to generate bubbles in order of 1 mm diameter to optimize the process. We measured significantly smaller bubbles at micro-scale orifices compared with submillimeter ones. However, the bubble sizes

generated from micro-orifices were still at least 0.4 mm to 0.8 mm above the optimal value of 1 mm in the investigated range of the gas flow rate.

From the quasi-static balance of forces, we learned that, the bubble size is directly proportional to the third root of the orifice diameter. Hence, if an attempt is made to reduce the bubble size to half, the orifice size should be reduced by one-eighth of the original value. Despite the manufacturing difficulties, this would significantly influence the mechanism of bubble formation as the capillary pressure and the gas kinetic energy would increase dramatically. Consequently, excessive pressure will build up in the gas chamber, which results in merging several bubbles in the vicinity above the orifice and finally generating relatively large bubbles. Hence, it is necessary to study the mechanism of bubble formation and detachment at micro-orifices to be able to define the feasibility and limitations of these orifices in case of bubble formation.

NOMENCLATURE

A	available surface area, cm^2/s
Bo	Bond number, $Bo = \rho_L d_{OR}^2 g/\sigma_L$
d_{OR}	orifice diameter , µm
E_0	specific energy, Wh/m^4
Fr	Froude number, $Fr = U_G^2/(d_{OR} g)$
g	gravity acceleration, m/s^2
h_D	hydrostatic height, m
K_L	mass transfer coefficient, cm/s
L	needle length, mm
N_C	capacitance number, $N_c = 4V_C \rho_L g/(\pi d_{OR}^2 P_H)$
N_W	gas flow rate number, $N_W = BoFr^{0.5}$
OTR	oxygen transfer rate, kgo_2/d
P	power, W
P_H	hydrostatic pressure, Pa
Δp	pressure drop, mbar
Q	standard gas flow rate through the orifice, smL/min
Q_C	critical gas flow, m^3/s
SOTE	standard oxygen transfer efficiency, %
T	diffuser thickness, µm
U_G	gas velocity through the orifice, m/s
V_C	gas chamber volume, m^3
V_F	Fritz bubble volume, m^3, $V_F = \pi \sigma_L d_{OR}/\rho_L g$
We	Weber Number, $We = U_G^2 d_{OR} \rho_G/\sigma_L$
We_Q^c	critical Weber Number, $We_Q^c = (\frac{16}{3})^{1/3} Bo^{-2/3}$
Υ	exponent
ρ_L	liquid density, kg/m^3
σ_L	liquid surface tension, N/m

ACKNOWLEDGMENT:

The work of Mr. Ehsan Mohseni is funded by the European Social Fund and the Free State of Saxony. Moreover, the contributions by Mr. Herrmann-Heber and Dr. Reinecke were

funded by the Ministry for Climate Protection, Environment, Agriculture, Conservation and Consumer Protection of the State of North Rhine-Westphalia (MULNV, LANUV NRW; reference number: 17-04.02.01-9a/2014).

REFERENCES

[1] C. Qu, Y. Yu, J. Zhang, Experimental study of bubbling regimes on submerged micro-orifices, International Journal of Heat and Mass Transfer 111 (2017) 17-28.
[2] Y.T. Kang, T. Nagano, T. Kashiwagi, Visualization of bubble behavior and bubble diameter correlation for NH3–H2O bubble absorption, International journal of refrigeration 25 (2002) 127-135.
[3] R. Lau, R. Mo, W.S.B. Sim, Bubble characteristics in shallow bubble column reactors, Chemical Engineering Research and Design 88 (2010) 197-203.
[4] C. Ribeiro Jr, P. Lage, Experimental study on bubble size distributions in a direct-contact evaporator, Brazilian journal of chemical engineering 21 (2004) 69-81.
[5] P. Painmanakul, K. Loubiere, G. Hebrard, P. Buffière, Study of different membrane spargers used in waste water treatment: characterisation and performance, Chemical Engineering and Processing: Process Intensification 43 (2004) 1347-1359.
[6] W.B. Zimmerman, V. Tesař, H.H. Bandulasena, Towards energy efficient nanobubble generation with fluidic oscillation, Current Opinion in Colloid & Interface Science 16 (2011) 350-356.
[7] L.K. Wang, N.K. Shammas, Y.-T. Hung, Advanced biological treatment processes, Springer Science & Business Media2010.
[8] N. Kantarci, F. Borak, K.O. Ulgen, Bubble column reactors, Process Biochemistry 40 (2005) 2263-2283.
[9] B. Jin, P. Yin, P. Lant, Hydrodynamics and mass transfer coefficient in three-phase air-lift reactors containing activated sludge, Chemical Engineering and Processing: Process Intensification 45 (2006) 608-617.
[10] M. Motarjemi, G. Jameson, Mass transfer from very small bubbles—the optimum bubble size for aeration, Chemical Engineering Science 33 (1978) 1415-1423.
[11] A. Hasanen, P. Orivuori, J. Aittamaa, Measurements of local bubble size distributions from various flexible membrane diffusers, Chemical Engineering and Processing: Process Intensification 45 (2006) 291-302.
[12] A.-E. Sommer, M. Wagner, S. Reinecke, M. Bieberle, F. Barthel, U. Hampel, Analysis of activated sludge aerated by membrane and monolithic spargers with ultrafast X-ray tomography, Flow Measurement and Instrumentation (2016).
[13] R. Kumar, N. Kuloor, The formation of bubbles and drops, Advances in chemical engineering 8 (1970) 255-368.
[14] A.A. Kulkarni, J.B. Joshi, Bubble formation and bubble rise velocity in gas− liquid systems: a review, Industrial & Engineering Chemistry Research 44 (2005) 5873-5931.
[15] D. McCann, R. Prince, Regimes of bubbling at a submerged orifice, Chemical Engineering Science 26 (1971) 1505-1512.
[16] W. Fritz, Berechnung des maximalvolume von dampfblasen, Phys. Z. 36 (1935) 379-388.
[17] H.N. Oguz, A. Prosperetti, Dynamics of bubble growth and detachment from a needle, Journal of Fluid Mechanics 257 (1993) 111-145.

[18] R. Bolaños-Jiménez, A. Sevilla, C. Martínez-Bazán, J. Gordillo, Axisymmetric bubble collapse in a quiescent liquid pool. II. Experimental study, Physics of Fluids 20 (2008) 112104.
[19] H. Tsuge, Hydrodynamics of bubble formation from submerged orifices, Encyclopedia of fluid mechanics 3 (1986) 191-232.
[20] A. Kupferberg, G. Jameson, Bubble formation at a submerged orifice above a gas chamber of finite volume, TRANSACTIONS OF THE INSTITUTION OF CHEMICAL ENGINEERS AND THE CHEMICAL ENGINEER 47 (1969) T241-+.
[21] Y. Park, A.L. Tyler, N. de Nevers, The chamber orifice interaction in the formation of bubbles, Chemical Engineering Science 32 (1977) 907-916.
[22] H. Tsuge, S.-I. Hibino, Bubble formation from an orifice submerged in liquids, Chemical Engineering Communications 22 (1983) 63-79.
[23] K. Terasaka, H. Tsuge, Bubble formation at a single orifice in highly viscous liquids, Journal of Chemical Engineering of Japan 23 (1990) 160-165.
[24] J. Mueller, W.C. Boyle, H.J. Popel, Aeration: principles and practice, CRC press2002.
[25] S.S. Sadhal, P.S. Ayyaswamy, J.N. Chung, Transport phenomena with drops and bubbles, Springer Science & Business Media2012.
[26] T. Tadaki, S. Maeda, The size of bubbles from single orifices, Kagaku Kogaku 27 (1963) 147-155.
[27] T. Takahashi, Bubble volume formed at submerged nozzles: constant flow condition, Kagaku Kogaku Ronbunshu 2 (1976) 138-143.
[28] K. Terasaka, H. Tsuge, Bubble formation under constant-flow conditions, Chemical Engineering Science 48 (1993) 3417-3422.
[29] S. Vafaei, P. Angeli, D. Wen, Bubble growth rate from stainless steel substrate and needle nozzles, Colloids and Surfaces A: Physicochemical and Engineering Aspects 384 (2011) 240-247.
[30] S. Vafaei, T. Borca-Tasciuc, D. Wen, Theoretical and experimental investigation of quasi-steady-state bubble growth on top of submerged stainless steel nozzles, Colloids and Surfaces A: Physicochemical and Engineering Aspects 369 (2010) 11-19.
[31] S. Vafaei, D. Wen, Bubble formation on a submerged micronozzle, Journal of colloid and interface science 343 (2010) 291-297.
[32] J. Xie, X. Zhu, Q. Liao, H. Wang, Y.-D. Ding, Dynamics of bubble formation and detachment from an immersed micro-orifice on a plate, International Journal of Heat and Mass Transfer 55 (2012) 3205-3213.
[33] X. Zhu, J. Xie, Q. Liao, R. Chen, H. Wang, Dynamic bubbling behaviors on a micro-orifice submerged in stagnant liquid, International Journal of Heat and Mass Transfer 68 (2014) 324-331.
[34] J.A. Simmons, J.E. Sprittles, Y.D. Shikhmurzaev, The formation of a bubble from a submerged orifice, European Journal of Mechanics-B/Fluids 53 (2015) 24-36.
[35] J. Zhang, Y. Yu, C. Qu, Y. Zhang, Experimental study and numerical simulation of periodic bubble formation at submerged micron-sized nozzles with constant gas flow rate, Chemical Engineering Science 168 (2017) 1-10.
[36] A.A. Alkhalidi, R. Amano, Factors affecting fine bubble creation and bubble size for activated sludge, Water and Environment Journal 29 (2015) 105-113.
[37] R.J. Benzing, J.E. Myers, Low frequency bubble formation at horizontal circular orifices, Industrial & Engineering Chemistry 47 (1955) 2087-2090.
[38] T. Ziegenhein, Fluid dynamics of bubbly flows, (2016).
[39] J. Canny, A computational approach to edge detection, IEEE Transactions on pattern analysis and machine intelligence (1986) 679-698.
[40] J. Daly, S. Patel, D. Bukur, Measurement of gas holdups and sauter mean bubble diameters in bubble column reactors by dynamics gas disengagement method, Chemical engineering science 47 (1992) 3647-3654.

[41] H. Yasuda, J. Lin, Small bubbles oxygenation membrane, Journal of applied polymer science 90 (2003) 387-398.
[42] W.B. Hayes, B.W. Hardy, C.D. Holland, Formation of gas bubbles at submerged orifices, AIChE Journal 5 (1959) 319-324.
[43] K. Loubière, G. Hébrard, Bubble formation from a flexible hole submerged in an inviscid liquid, Chemical engineering science 58 (2003) 135-148.
[44] H.J. Pöpel, M. Wagner, Modelling of oxygen transfer in deep diffused-aeration tanks and comparison with full-scale plant data, Water Science and Technology 30 (1994) 71.